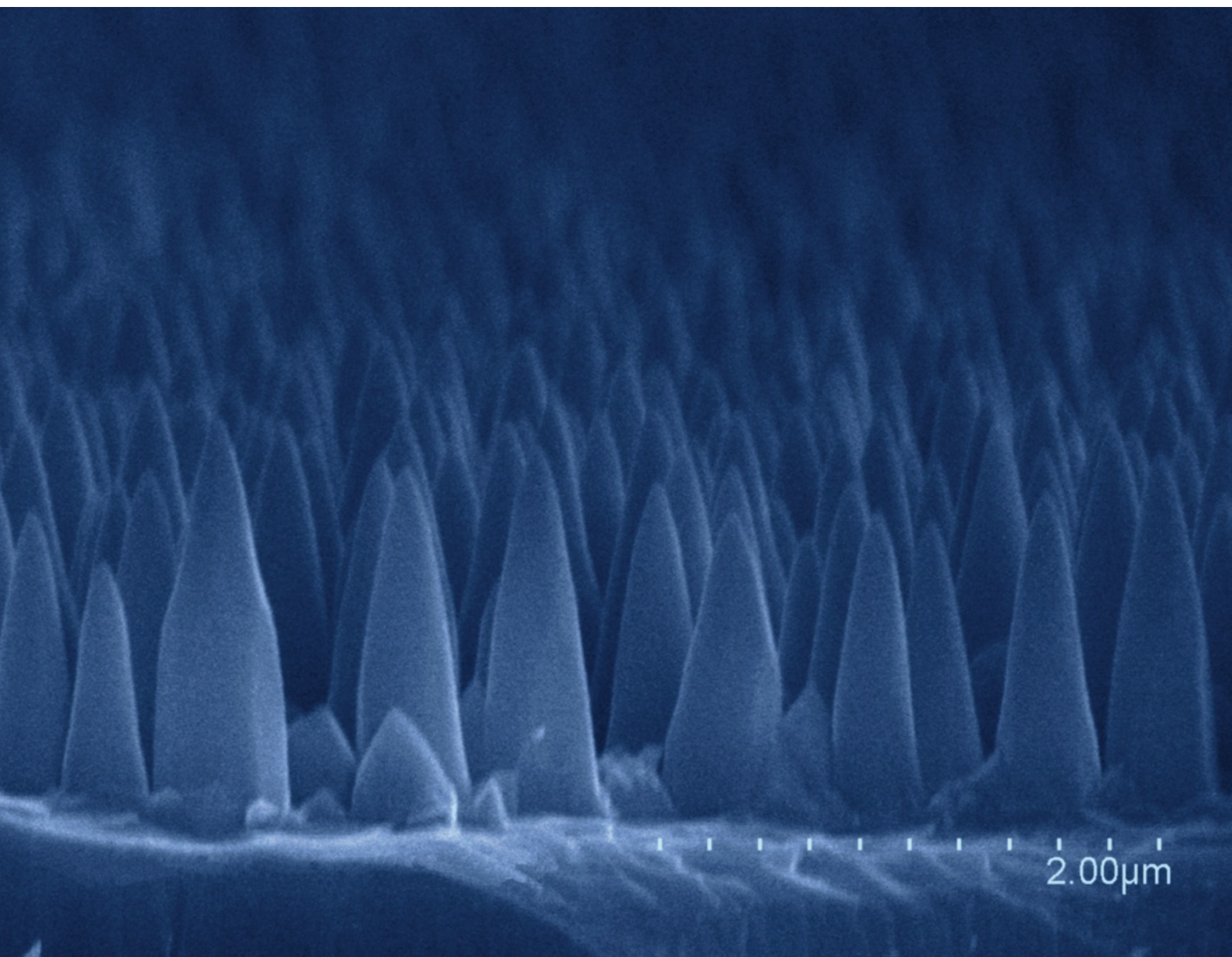# physica p s s ᶜ status solidi

current topics in solid state physics

**10
2013**

Growth of "moth-eye" ZnO nanostructures on Si(111), c-Al₂O₃, ZnO and steel substrates

V. E. Sandana, D. J. Rogers, F. Hosseini Teherani, P. Bove, M. Molinari, M. Troyon, A. Largeteau, G. Demazeau, C. Scott, G. Orsal, H.-J. Drouhin, A. Ougazzaden, and M. Razeghi

2.00µm

physica **pss** status solidi c

www.pss-c.com

current topics in solid state physics

Growth of "moth-eye" ZnO nanostructures on Si(111), c-Al$_2$O$_3$, ZnO and steel substrates by pulsed laser deposition

Vinod E. Sandana[1], David J. Rogers[1], Ferechteh Hosseini Teherani[1], Philippe Bove[1], Michael Molinari[2], Michel Troyon[2], Alain Largeteau[3], Gérard Demazeau[3], Colin Scott[4], Gaelle Orsal[5], Henri-Jean Drouhin[6], Abdallah Ougazzaden[7], and Manijeh Razeghi[8]

[1] Nanovation, 103b rue de Versailles, 91400 Orsay, France

[2] LMEN, Université de Reims Champagne-Ardennes, 21 rue Clement Ader, 51685 Reims France

[3] ICMCB-CNRS, Bordeaux 1 University (Science & Technology), 87 Av. A. Schweitzer, 33608 Pessac, France

[4] Arcelor-Mittal Basic Research, Voie Romaine, 57283 Maizières-les-Metz, Metz, France

[5] LMOPS, UMR CNRS 7132, Université de Metz and SUPELEC, 2 rue E. Belin, 57070 Metz, France

[6] Department of Irradiated Solids, École Polytechnique, 91128 Palaiseau, France

[7] Georgia Institute of Technology/GT-Lorraine-UMI 2958 Georgia Tech-CNRS, 2-3 rue Marconi, 57070 Metz, France

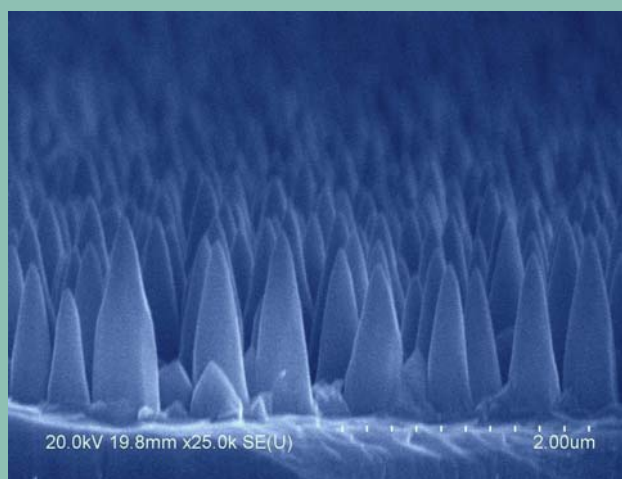[8] Center for Quantum Devices, ECE Department, Northwestern University, Evanston, Illinois 60208, USA

Self-forming, vertically-aligned, arrays of black-body-like ZnO moth-eye nanostructures were grown on Si(111), c-Al$_2$O$_3$, ZnO and high manganese austenitic steel substrates using Pulsed Laser Deposition. X-ray diffraction (XRD) revealed the nanostructures to be well-crystallised wurtzite ZnO with strong preferential c-axis crystallographic orientation along the growth direction for all the substrates. Cathodoluminescence (CL) studies revealed emission characteristic of the ZnO near band edge for all substrates. Such moth-eye nanostructures have a graded effective refractive index and exhibit black-body characteristics. Coatings with these features may offer improvements in photovoltaic and LED performance. Moreover, since ZnO nanostructures can be grown readily on a wide range of substrates it is suggested that such an approach could facilitate growth of GaN-based devices on mismatched and/or technologically important substrates, which may have been inaccessible till present.

SEM side view of ZnO nanocones grown on Si(111).

1 Introduction

ZnO is a remarkable multifunctional material with a distinctive set of properties including a direct bandgap of ~3.4 eV and an exciton binding energy of ~60 meV. It also has a high transparency over the visible spectrum, a strong piezoelectric response, a very wide range of tuneable conductivities (varying from semi-insulating to semi-metallic) and good biocompatibility [1]. In previous works [2, 3] it was shown that Pulsed Laser Deposition (PLD) could be used to give self-forming arrays of vertically

aligned nanostructures on Si and sapphire substrates. In particular, moth-eye-type nanostructures were shown to exhibit blackbody-like properties over the whole visible spectrum [4], which suggested that they could be used, for instance, as anti-reflection coatings on solar cells [5] or for enhanced extraction in LEDs [6]. Such nanocones were also used as a template for MOVPE GaN regrowth [7] and as an active layer in n-ZnO/p-Si heterojunction LEDs [8]. This paper reports on the development of similar ZnO structures on ZnO and high manganese austenitic steel substrates by PLD and compares them with those obtained on Si(111) and c-Al$_2$O$_3$.

2 Experiments and results
2.1 Experiments

ZnO moth-eye nanostructures were grown by PLD on Si(111), c-Al$_2$O$_3$, hydrothermal ZnO [9] and austenitic steel substrates, using growth conditions described previously [8] ZnO nanostructures were grown from a 99.99% pure ZnO target by PLD using a KrF excimer laser (248 nm). The chamber was evacuated using a turbo-molecular pump to a background vacuum of about 1×10^{-6} Torr with or without Ar as a background gas. The growth conditions were: laser frequency of 10 Hz, substrate temperature was 700 °C, growth times of 10 min. These conditions were similar for all substrates. Sample morphology was studied using a Hitachi S4800 Field Emission-Scanning Electron Microscope (FE-SEM). The crystal quality of the nanostructures was investigated using high resolution X-Ray Diffraction (XRD) performed in a Panalytical MRD Pro system using Cu Kα radiation Room temperature Cathodoluminescence (CL) was performed with a home made system in an SEM [10] in order to study the optical properties and gain insight into impurity and defect density.

2.2 Results

Figure 1 shows SEM images of samples of ZnO nanocones obtained on the 4 different substrates. The structures on all the substrates exhibit dense, self-forming, arrays of vertically-aligned cone-like "moth-eye" nanostructures.

Laudise and Ballman [11] suggest that such tapered nanorods develop as a result of the relative growth rates of the different crystal facets of ZnO (growth rates are higher for directions orthogonal to closer spaced lattice planes). For wurtzite ZnO, the maximum growth rate is in the [0001] direction and it should be about twice as fast as that in the [10-10] direction, while the growth rate along [10-11] should be intermediate. Figure 2 shows a top view of ZnO nanocones on a Si(111) substrate.

In this figure the characteristic, six-fold, faceting of the wurtzite ZnO structure can clearly be discerned the lack of such faceting in the smoothed, nanocone-like appearance observed in Fig. 1 is most probably an illusion due to a surface transparency induced by the higher SEM accelerating voltage used for these acquisitions.
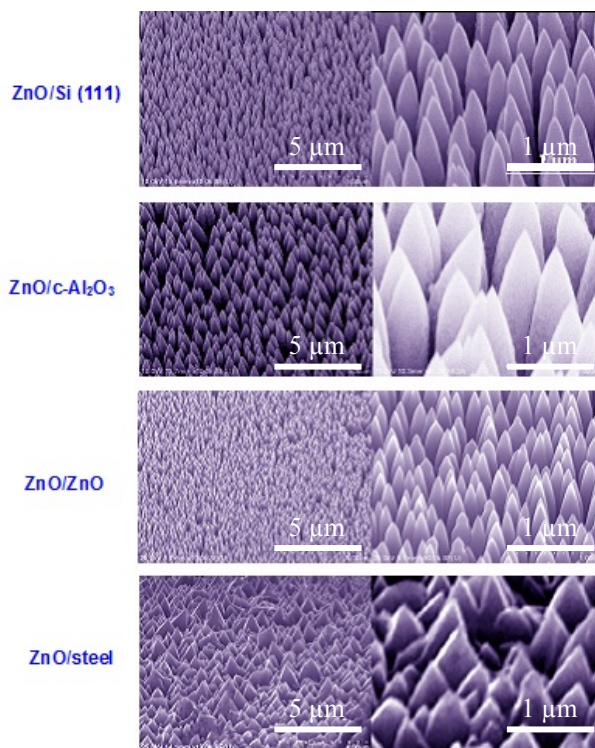

Figure 1 SEM images of ZnO nanostructures grown by PLD on (a) Si(111), (b) c-Al$_2$O$_3$, (c) ZnO and (d) high manganese austenitic steel. The images on the right are zooms of the images on the left. The scales for the images on the right are similar for all substrates.
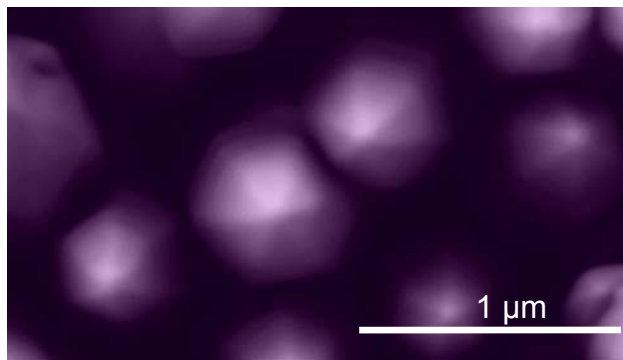

Figure 2 SEM top view of ZnO nanocones grown on Si(111).

Figure 3 shows the XRD 2θ/ω scans for the (0002) peaks of the nanostructures grown on the different substrates. Strong ZnO (0002) reflections corresponding to a c-axis oriented wurtzite phase were observed for all the samples. The Full Width at Half Maximum (FWHM) for the samples (see Table 1) from 0.011° for the nanocones grown on ZnO up to 0.019 on Si, 0.06° on c-Al$_2$O$_3$ and 0.34° on steel. This suggests that, apart from the ZnO on steel, the nanostructures have relatively small variation in lattice parameter relative to that observed for ZnO thin

films on similar substrates. These results indicate that the sample grown on ZnO bulk was more perfectly crystallized than the others.
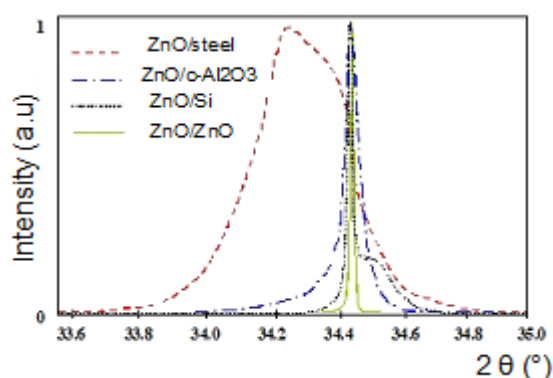

Figure 3 Normalised XRD 2θ/ω scans (linear intensity scale) for the (0002) peaks of the nanostructured ZnO grown on various substrates.

Table 1 also shows that the main peak position in the 2θ/ω scans is similar for the Si, c-Al$_2$O$_3$ and ZnO substrates, corresponding to c-lattice parameters of 5.202-5.203 Å. This is very close to what would be expected for relaxed wurtzite ZnO (5.204–5.206 Å). The c-lattice parameter corresponding to the peak maximum for the nano ZnO on high manganese austenitic steel, however, is significantly larger, at 5.225 Å, which corresponds to ZnO under compressive strain (the lattice parameter of the steel is 3.6137 Å). Closer inspection reveals that the peak seems to be made up of multiple peaks, which could be related to relaxation during film growth.

Table 1 Comparison of XRD scan intensities and FWHM for ZnO nanocones grown on Si(111), c-Al$_2$O$_3$, ZnO and high Mn austenitic steel.

substrate	ω scan intensity (cps)	ω rocking curve FWHM (º)	2θ/ω FWHM (°)	c lattice parameter (Å)
Si (111)	~1000	0.85	0.019	5.203
c-Al$_2$O$_3$	~500	0.94	0.06	5.202
bulk ZnO	~100000	0.028	0.011	5.202
austenitic steel	~100	11.7	0.34	5.225

The nano ZnO/Si(111) shows broadening on the higher-angle side at the base of the peak, signifying a region with a smaller c-lattice parameter. This could be due to disorder at the start of growth creating a less dense a-b plane at the base of the nanocones (and thus a larger a-lattice parameter). Figure 4 shows an SEM side-view image, which confirms that crystallographic disorder does indeed exist at the base of the cones.
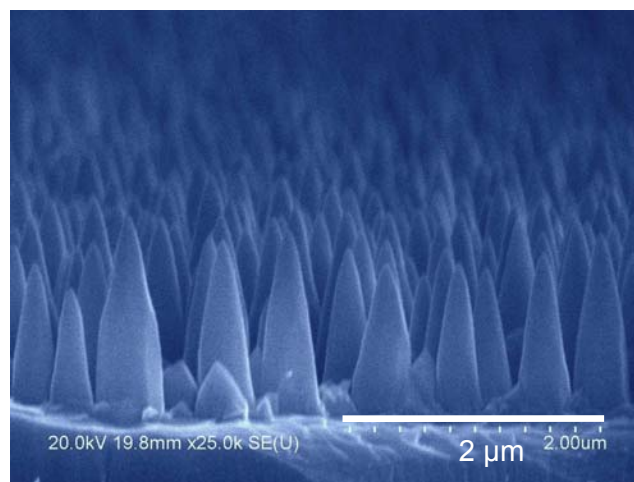

Figure 4 SEM side view of ZnO nanocones grown on Si (111).

The XRD ω rocking curves (open detector configuration) are shown in Fig. 5.
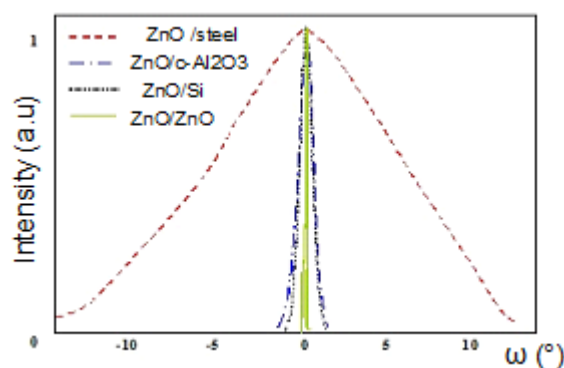

Figure 5 Normalised XRD ω scan rocking curves (linear intensity scale) for the (0002) peaks of the nanostructured ZnO grown on various substrates.

The FWHM of the rocking curve is significantly larger for the sample on steel and is narrowest for the sample on ZnO (a lower FWHM corresponds to a smaller dispersion in the crystallographic orientation). The FWHM of the rocking curve of ZnO on sapphire is larger than typically be observed for equivalent thin films whereas that for Si is comparable or smaller.

RT CL spectra of the nanostructured ZnO on various substrates are shown in Fig. 6 and Table 2.
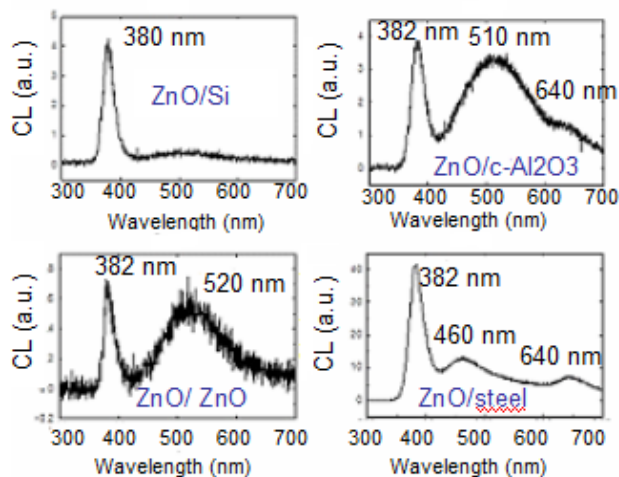

Figure 6 CL spectra of the nanostructured ZnO on various substrates.

Table 2 Comparison of CL spectra, main peak, FWHM, and intensity for ZnO nanostructures grown on Si(111), c-Al2O3, ZnO and high Mn austenitic steel.

substrate	1st peak position (nm)	1st peak FWHM (nm)	2nd peak position (nm)	3rd peak position (nm)
Si (111)	380	22	none	none
c-Al$_2$O$_3$	382	23	510	640
bulk ZnO	382	22	520	None
austenitic steel	382	28	460	640

The spectra all show an ultraviolet (UV) band (at around 380-382 nm), which is characteristic of Near Band Edge (NBE) emission from wurtzite ZnO [12]. The NBE emission wavelength and the FWHM were slightly lower for the structures grown on the Si(111) substrates than for those grown on the c-Al$_2$O$_3$, ZnO and austenitic steel. Green bands visible in the spectra for the growths on c-Al$_2$O$_3$ and bulk ZnO (at wavelengths of 510 and 520 nm, respectively) were attributed to defects in the ZnO [13]. A red peak at 640 nm, present in the spectra for the growths on c-Al$_2$O$_3$ and steel, could be related to Al and Fe from the substrates diffusing into the ZnO. An additional blue (460 nm) peak was observed in the spectrum for the sample on steel. Although the origin is not yet clear, a similar band has been reported elsewhere for ZnO films [14] and nanorods [15]. Jin et al. [16] considered that it might be due to the existence of oxygen-depleted interface traps. Of particular note, is the absence of green, red or blue bands

in the CL spectra of the ZnO nanocones grown on Si(111), plus the relatively intense peak of the NBE. These indicate that the nanostructures on Si had particularly good crystal quality and a relatively low defect density.

3 Conclusion

Nanostructures were grown on Si(111), c-Al$_2$O$_3$, ZnO and high Mn austenitic steel substrates using catalyst-free PLD. The impact of substrates on the sample morphology and crystallographic and optical properties was investigated. Self-forming, vertically-aligned, arrays of moth-eye-like nanocones were obtained on all substrates. XRD and RT CL studies indicated that the nanostructures grown on all substrates were highly c-axis oriented wurtzite ZnO with strong NBE emission. Of particular note was the fact that the ZnO crystallised well on all substrates (including steel) and that the moth-eye structures on Si(111) showed very good crystallographic and optical characteristics compared with equivalent thin films grown on Si.

Such moth-eye nanostructures have a graded effective refractive index and exhibit black-body characteristics. In photovoltaic applications they may, therefore, have potential for use as anti-reflective coatings [4], light trapping layers and nanostructured template back-electrodes [17]. In LED applications they may have potential for use as coatings for enhancement of light extraction6, as active ZnO layers for light emission [9] or as nanostructured templates for (In)GaN regrowth [7]. Indeed, since ZnO nanostructures can be grown readily on a wide range of substrates such an approach could facilitate growth of GaN-based devices and nanostructures on mismatched and/or technologically important substrates, which may have been inaccessible till present, including steel, have been inaccessible till present, including steel.

References
[1] D.C. Look, in: Zinc Oxide: A Material for Micro- and Opto-electronic Applications, edited by N. H. Nickel, eNATO Science series II: Mathematics, Physics and Chemistry, 194 37 (2005).
[2] V. E. Sandana, D. J. Rogers, F. Hosseini Teherani, R. McClintock, M. Razeghi, H.-J. Drouhin, M.C. Clochard, V. Sallet, G. Garry, and F. Fayoud, Proc. SPIE **6895**, 68950Z (2008).
[3] V. E. Sandana, D. J. Rogers, F. Hosseini Teherani, R. McClintock, C. Bayram, M. Razeghi, H.-J. Drouhin, M.C. Clochard, V. Sallet, G. Garry, and F. Falyouni, J. Vac. Sci. Technol. B **27**, 31678-1683 (2009).
[4] M. Peres, M. J. Soares, A. J. Neves, T. Monteiro, V. E. Sandana, F. Teherani, and D. J. Rogers, Phys. Status Solidi A **247**(7), 1695–1698 (2010).
[5] L. Tsakalakos, Mater. Sci. Eng. R **62**, 175–189 (2008).

[6] J. Zhong, H. Chen, G. Saraf, Y. Lu, C. K. Choi, and J. J. Song, Appl. Phys. Lett. **90**, 203515 (2007).

[7] D. J. Rogers, V. E. Sandana, F. Hosseini Teherani, S. Gautier, G. Orsal, T. Moudakir, M. Molinari, M. Troyon, M. Peres, M. Soares, A. Neves, T. Monteiro, D. McGrouther, J. Chapman, H.-J. Drouhin, M. Razeghi, and A. Ougazzaden, Renew. Energy Environ., OSA PWB3 (2011).

[8] D. J. Rogers, V. E. Sandana F. Hosseini Teherani, M. Razeghi, and H.-J. Drouhin, Proc. SPIE **7217**, 721708 (2008).

[9] D. J. Rogers, F. Hosseini Teherani, A. Largeteau, G. Demazeau, C. Moisson, D. Turover, J. Nause, G. Garry, R. Kling, T. Gruber, A. Waag, F. Jomard, P. Galtier, A. Lusson, T. Monteiro, M. J. Soares, A. Neves, M. C. Carmo, M. Peres, G. Lerondel, and C. Hubert, Appl. Phys. A **88**, 49-56 (2007).

[10] M. Troyon, D. Pastré, J.P. Jouart, and J. L. Beaudoin, Ultramicroscopy **75**, 15 (1998).

[11] R. A Laudies and A. Ballman, J. Phys. Chem. **64**, 688 (1960).

[12] Y. C. Kong, D. P. Yu, B. Zhang, W. Fang, and S. Q. Feng, Appl. Phys. Lett. **78**, 407 (2001).

[13] S. A. Studenikim, N. Golego, and M. J. Cocivera, J. Appl. Phys. **84**, 2287 (1998).

[14] Z. Fu, B. Lin, G.Liao, and Z. Wu J. Cryst. Growth **193**, 316 (1998).

[15] J.-J. Wu and S. C. Liu, Adv. Mater. **14**, 215 (2002).

[16] B. J. Jin, S. Im, and S. Y. Lee, Thin Solid Films **366**, 107 (2000).

[17] T. Söderström, D. Dominé, A. Feltrin, M. Despeisse, F. Meillaud, G. Bugnon, M. Boccard, P. Cuony, F.-J. Haug, S. Faÿ, S. Nicolay, and C. Ballif, Proc. SPIE **7603** (2010).